Texture of Rotary-Friction-Welded from Dissimilar Medium Carbon Steels

Zakaria Boumerzoug, Elena Priymak, Anna Stepanchukova, Anne-Laure Helbert, François Brisset, Thierry Baudin

World Journal of Condensed Matter Physics, 2020, 10, 178-190
https://www.scirp.org/journal/wjcmp
ISSN Online: 2160-6927
ISSN Print: 2160-6919

Texture of Rotary-Friction-Welded from Dissimilar Medium Carbon Steels

Zakaria Boumerzoug[1*], Elena Priymak[2], Anna Stepanchukova[3], Anne-Laure Helbert[4], François Brisset[4], Thierry Baudin[4]

[1]Department of Mechanical Engineering, LMSM, University of Biskra, Biskra, Algeria
[2]Orenburg State University, Orenburg, Russia
[3]ZBO Drill Industries, Orenburg, Russia
[4]Université Paris-Saclay, CNRS, Institut de chimie moléculaire et des matériaux d'Orsay, Orsay, France
Email: *zboumerzoug@yahoo.fr, e.prijmak@zbo.ru, annastep56@zbo.ru, anne-laure.helbert@universite-paris-saclay.fr, francois.brisset@universite-paris-saclay.fr, thierry.baudin@universite-paris-saclay.fr

How to cite this paper: Boumerzoug, Z., Priymak, E., Stepanchukova, A., Helbert, A.-L., Brisset, F. and Baudin, T. (2020) Texture of Rotary-Friction-Welded from Dissimilar Medium Carbon Steels. *World Journal of Condensed Matter Physics*, **10**, 178-190.
https://doi.org/10.4236/wjcmp.2020.104011

Received: August 26, 2020
Accepted: November 15, 2020
Published: November 18, 2020

Abstract

The purpose of the present study was to investigate the texture in dissimilar medium carbon steels welded by rotary friction technique. The Electron Backscatter Diffraction (EBSD) technique was the main technique used to investigate the effect of welding on grain size and grain crystallographic orientation in the welded joint. Moreover, the effect of isothermal heat treatment at 600˚C on welded joint has been studied knowing that this annealing allows to decrease the residual stresses. EBSD results revealed different subzones in welded joint. The texture in the weld is essentially composed of three components: Goss {110} <001>, Rotated Cube {100} <110>, and Rotated Goss {110} <110> orientation. The heat treatments applied on welded material had a slight effect on texture and grain size.

Keywords

Texture, Rotary Friction Welding, Medium Carbon Steels

1. Introduction

This Friction welding is a solid state welding method. This type of welding involves the union between a stationary and a rotating member, due to the friction heat generated while undergoing high normal forces at the interface, below the melting temperature, the welded joint is achieved [1] [2]. In the case of joining circular bars, including pipes, the rotary friction welding (RFW) method is used. This technology has a lot of advantages over other welding processes. These ad-

vantages are; no melting, high reproducibility, short production time, low energy input, limited heat affected zone, avoidance of porosity formation, and no grain growth and the use of non-shielding gasses during welding process [3] [4] [5].

During welding by RFW, rapid heating and cooling take place, which produces severe thermal cycle near weld line. Along the axial direction, three main zones can be observed from the line contact: Welding zone (WZ), thermal mechanical affected zone (TMAZ) and heat affected zone (HAZ). The TMAZ is the zone where heat transfers from the weld metal to the base metal. As a result, the welded joint obtained by RFW is a structurally inhomogeneous zone, characterized by a wide spectrum of formed structures and stresses [6].

Friction welding (FW) is an economical and environmental friendly solid state joining process which is applied to join similar as well as dissimilar ferrous and nonferrous materials [7]. Literature shows that RFW technique has been effectively applied to join dissimilar steels, such as carbon steel AISI 1020 and ductile iron ASTM A536 [8], AISI 304 austenitic stainless steel and AISI D3 tool steel [9]. In the most published works, the main objective was focused on investigation of the effects of process parameters such as rotational speed and friction time on the microstructure and mechanical properties of the friction welded. For example, Zdemira *et al.* [10] have investigated the influence of rotational speed on the mechanical and structural properties of the plastically deformed zone at the interface of the weld during friction welding of two different steels (AISI 304L to AISI 4340 alloy steel). It was found that the tensile strength increases with increasing the rotational speed. Radosław *et al.* [8] studied the effect of RFW parameters on tensile strength and microstructural properties of dissimilar joints in carbon steel AISI 1020 and ductile iron ASTM A536. It was found that as the friction force and the friction time increase, the tensile strength also increases. Haribabu *et al.* [9] investigated the weldability in the different combinations of AISI 304 austenitic stainless steel and AISI D3 tool steel using the RFW welding technique. The results showed that the tensile strength of the joints increases with the increase of the upsetting and friction force initially, and decreases after reaching the maximum value of 388 MPa.

However, crystallographic aspect of the welded joint remains a research question knowing that limited researches have been reported about the texture distribution in welded dissimilar joints by RFW [11] [12] but no investigation of texture in welded dissimilar steels joined by RFW process. For example, Gaikwad *et al.* [11] studied the texture of friction welded carbon steel (EN24) and nickel based superalloy (IN718). Electron Back Scattered Diffraction (EBSD) analysis showed substantial changes in high angle grain boundaries, low angle grain boundaries and twin boundaries in TMAZ and HAZ areas. Also significant refinement in grain size was observed at TMAZ with reference to base metals. Gan *et al.* [12] investigated by neutron diffraction the texture gradient around the weld line in RFW dissimilar metals of AA7020 Aluminium Alloy with 316L steel. The texture analysis showed a weak rotated Cube near the bond line of

AA7020-T6 side which indicated a plastic deformation of AA7020-T6 during welding. However, two very weak Cube and Goss components have been identified in the 316 L steel pole figures.

In the present study, investigation of RFW of the two dissimilar steels 32-2Mn and 40-Cr-Ni is important, because these two steels were used for the production of geological exploration drill pipes [13]. In previous investigations [13] [14], analysis was focused on the post-weld tempering effect on the mechanism of fracture of welded joints of these medium alloy steels [13], and the residual stress distribution [14]. Stress distribution in welded joint is characterized by high compressive stresses in thermomechanical affected zone, due to the microstructural changes present in the cross-section of the welds. However, the post heat treatments caused a relaxation phenomenon in weld region which is due to the recovery and recrystallization reactions [14].

However, investigation of the texture in rotary friction welded joints from these dissimilar materials has never been reported up-to-date. Furthermore, study and controlling texture are necessary because it affects mechanical properties. The nature of the texture developed in a particular specimen depends on the material and on the mechanical and thermal treatments [15].

In this context, the main objective of this research is to investigate the texture in dissimilar steels welded joint made by rotary friction welding and also to understand the heat treatment effect on the crystallographic texture which has not been studied before.

2. Experimental Procedure

2.1. Materials and Welding Process

Tow medium carbon steels were chosen to be welded by rotary friction technique, 32-2Mn and 40-Cr-Ni. The chemical composition of the welded materials is shown in **Table 1**.

Rotary friction welding was performed on pipe billets with a diameter of 63.5 mm and a wall thickness of 4.5 mm. Experimental samples were welded on a Thompson-60 friction welding machine in several stages. A rotary tube with a constant speed is pressed onto a stationary tube and the relative movement creates heat by friction. When the temperature necessary for formation of welded joint is reached at the interface, the two tubes start to deform plastically. After a certain short time, the forging phase begins, where the motion is stopped rapidly and the axial pressure is increased until the plastic deformation ceases.

In this investigation, the welding parameters were as follows: friction force 50 kN, forging force 130 kN, friction time 5.86 s, and rotation speed 800 rpm which

Table 1. The chemical composition of the welded materials.

Material	C	Mn	Si	S	P	Cr	Ni	Cu	Mo
32-2Mn	0.32	1.07	0.18	0.002	0.006	0.09	0.10	0.17	0.02
40-Cr-Ni	0.31	0.53	0.32	0.006	0.004	0.51	1.06	-	0.09

are chosen according to the previous works [13] [14]. As the melting temperature is not reached, this welding technique does not produce typical welding defects known from fusion welding [16].

2.2. Microstructure and Texture Analysis

The purpose of the EBSD experiments was to determine the texture before and after heat treatment at 600˚C for 1 min of the welded joint. Specimens were prepared for EBSD analysis in a standard manner (mechanical polishing with SiC paper and electro polishing with the A2 Struers solution during 12 s in 40 V flux 12). A Zeiss Sigma HD FEG-SEM operating at 20 kV coupled with the automatic OIM™ (Orientation Imaging Microscopy) software from TSL-EDAX Company was used for the sample cross section EBSD analyses. **Figure 1** presents the schematic illustration of the studied area. The pole figures were calculated, using the harmonic series expansion method (series rank L = 34), from the orientations *measured* by EBSD. Each orientation was modeled by a gaussian function with a 5˚ half width. The EBSD maps are measured in the (A1, A2) plane.

3. Results and Discussion

Figure 2 shows EBSD map of welded of 32-2Mn steel to 40-Cr-Ni steel by RFW process, before (**Figure 2(a)**) and after post-weld heat treatment at 600˚C (**Figure 2(b)**). The welded joint obtained by RFW is a structurally inhomogeneous zone. From this general view, weldment can be divided broadly into two zones, (1) Weld interface (WI) and/or thermo mechanically affected zone (TMAZ) on both sides. However, the HAZ cannot be distinguished from the BM. Based on the scale in **Figure 2(a)**, the thickness of WI is less than 500 μm. The microstructure in this region consists of fine grains with. The TMAZ is characterized by spiral lines. It has been reported that in RFW, the rotation and the axial force govern the plastic material flow that results in shear as well as compressive deformation. Therefore, the flow lines have a spiral shape [17].

As mentioned in our previous paper [14], the microstructure observations revealed the intensive development of dynamic recrystallization processes in the

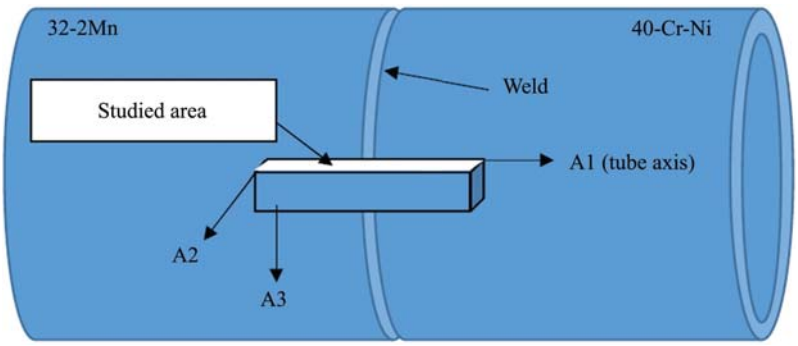

Figure 1. Schematic illustration of the EBSD studied area (A1-A2 plane in white) of samples with the coordinate system.

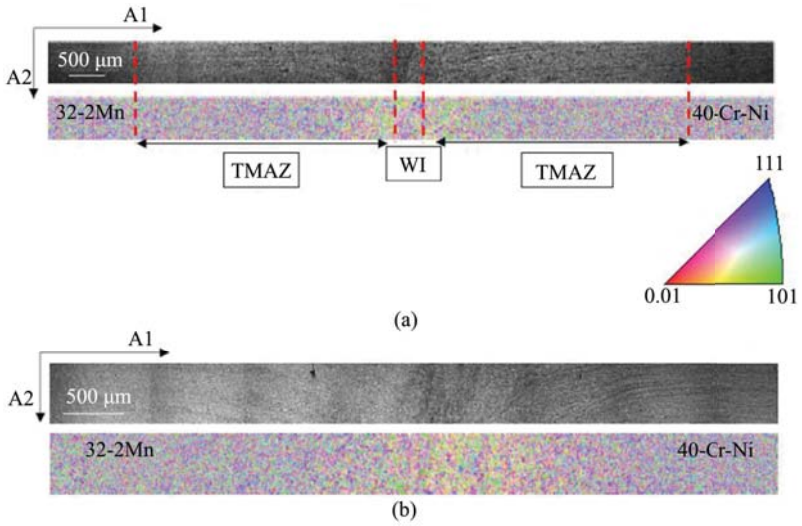

Figure 2. EBSD maps (QI and A3-IPF) of welded of 32-2Mn steel to 40-Cr-Ni steel by RFW process, (a) before and (b) after post-weld heat treatment at 600˚C. The color code is given on the standard triangle. (QI: The image quality parameter or IQ describes the quality of an electron backscatter diffraction pattern).

TMAZ of the both sides of the welded joint. This dynamic recrystallization reaction is due to heating and deformation during friction process. The color of individual grains in EBSD maps describes the {hkl} crystallographic plane parallel to the observation plane (**Figure 2(a)** and **Figure 2(b)**). These EBSD maps give a general idea about the grain morphology and orientation along the welded joint. From the EBSD maps of **Figure 2**, the microstructure of the center of the welded joint is characterized by coarse grains and the other zones (HAZ, BM) are composed of finer equiaxed-grains. The colored inverse pole figure (IPF) map of the welded joint is also presented in **Figure 2**. The color of each grain indicates its crystallographic direction parallel to A3 (red for {001}, blue for {111}, and green for {101}), as shown in the stereographic triangle.

For clarity, seven distinct sub-zones were considered in all welded joint (sub-zones a, b, c, d, e, f, and g) (**Figure 3**). The sub-zones (a) and (g) correspond to the two base metals which are not affected by the RFW process. The sub-zone (d) is the common zone (WI) of the dissimilar steels, and it is a mixture zone as shown in EDS profile of the welded joint (**Figure 4**), the chemical profiles of the two selected elements (Cr and Mn) change along this sub-zone WI. The sub-zones (c) and (e) are the adjacent zones to the mixture zone (d). From the EBSD maps, these sub-zones are different from the base metals and mixture zone. Besides, the (b) and (f) sub-zones are characterized by spiral lines.

Figure 5 presents the grain size distribution along welded joint before and after heat treatment at 600˚C. Grain size increases in the two sub-zones (c) and (e) and in the weld (sub-zone d). This is probably due to a dynamic recrystallization effect during welding. As observed in other materials welded by RFW, such as molybdenum [16]. It is well established in the literature that dynamic recrystallization occurs during FW [11] [18] [19]. In addition, there is a slight difference

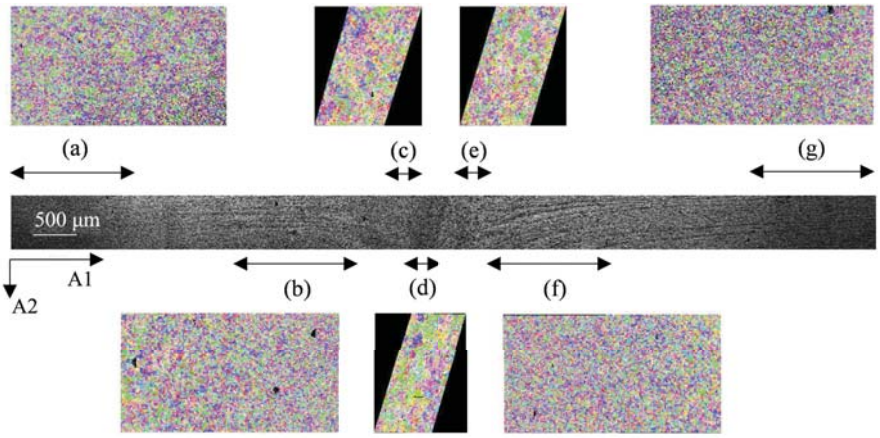

Figure 3. EBSD map of different sub-zones welded of 32-2Mn steel to 40-Cr-Ni steel by RFW process.

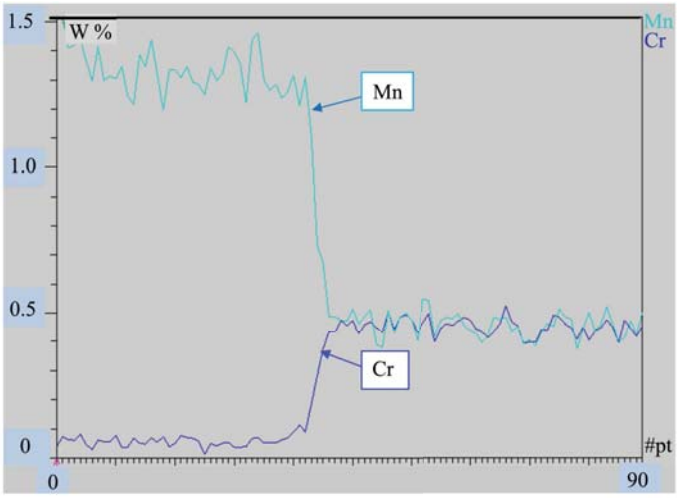

Figure 4. EDS profile along the common zone (WI) of the welded joint 32-2Mn steel/ 40-Cr-Ni steel by RFW process.

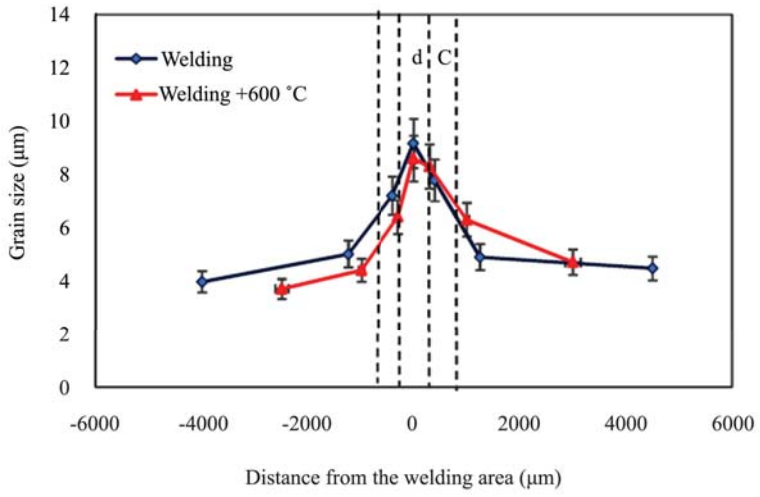

Figure 5. Grain size distribution along welded joint before and after heat treatment at 600˚C.

between the welded dissimilar steels before and after heat treatment at 600˚C, because the remaining time at 600˚C is very short (60 s). From mechanical aspect, this result is important, because this treatment did not cause any grain growth but it reduced the residual stresses as mentioned in our previous published work [14]. The stresses are less relaxed in the different zones (in the center of the welded and the TMAZ).

Besides, the fraction of high angle grain boundaries (HAGB) (>15˚) decreases in the two sub-zones (c) and (e) and in the weld (sub-zone d) (**Figure 6**) down to 75%. It is to be linked with the texture that shows up more grains in the same orientation (**Figure 3**) and therefore the misorientation between these grains is low. In comparison, with a random texture distribution of MacKenzie, the HAGB percentage is approximately 98%. More, Stütz *et al.* [16], found that due to the higher strain rates achieved in the contact zone, the production of dislocations was higher than in all other zones. Consequently, the magnitude of dynamic recrystallization was also higher and the formation of low angle grain boundaries was enhanced. For this reason, the percentage of HAGB in the contact zone (the center of the weld) is lower than in other zones of the welded joint.

In the welded zone, the grain size and percentage of HAGB are similar before and after heat treatment. On the contrary, the percentage of HAGB in base metal was observed to be 88% before heat treatment and 96% after heat treatment.

Figure 7 presents the pole figures of welded joint before heat treatment. It is necessary to mention that the maximum intensity of the pole figures was measured in the two sub-zones (c) and (e) and in the weld (sub-zone d) which confirms the crystallographic difference between the center of the welded joint and the other zones. The development of different texture in the welded joint is due to the microstructural heterogeneity of the welded joint. This heterogeneity can be explained by the welding of dissimilar steels and also by the formation of different sub-zones from the contact zone which is highly recrystallized to the base metal.

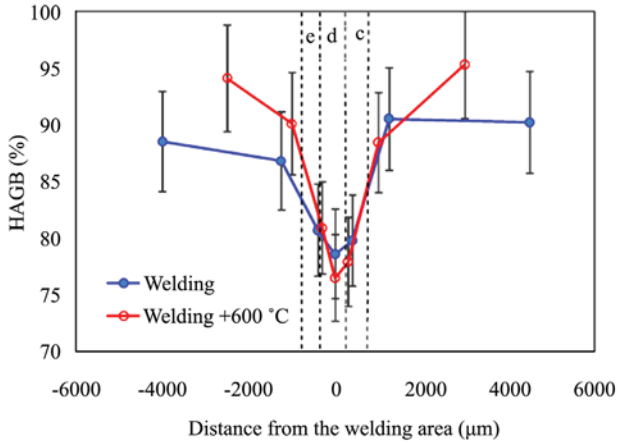

Figure 6. Fraction of HAGB distribution along welded joint before and after heat treatment at 600˚C.

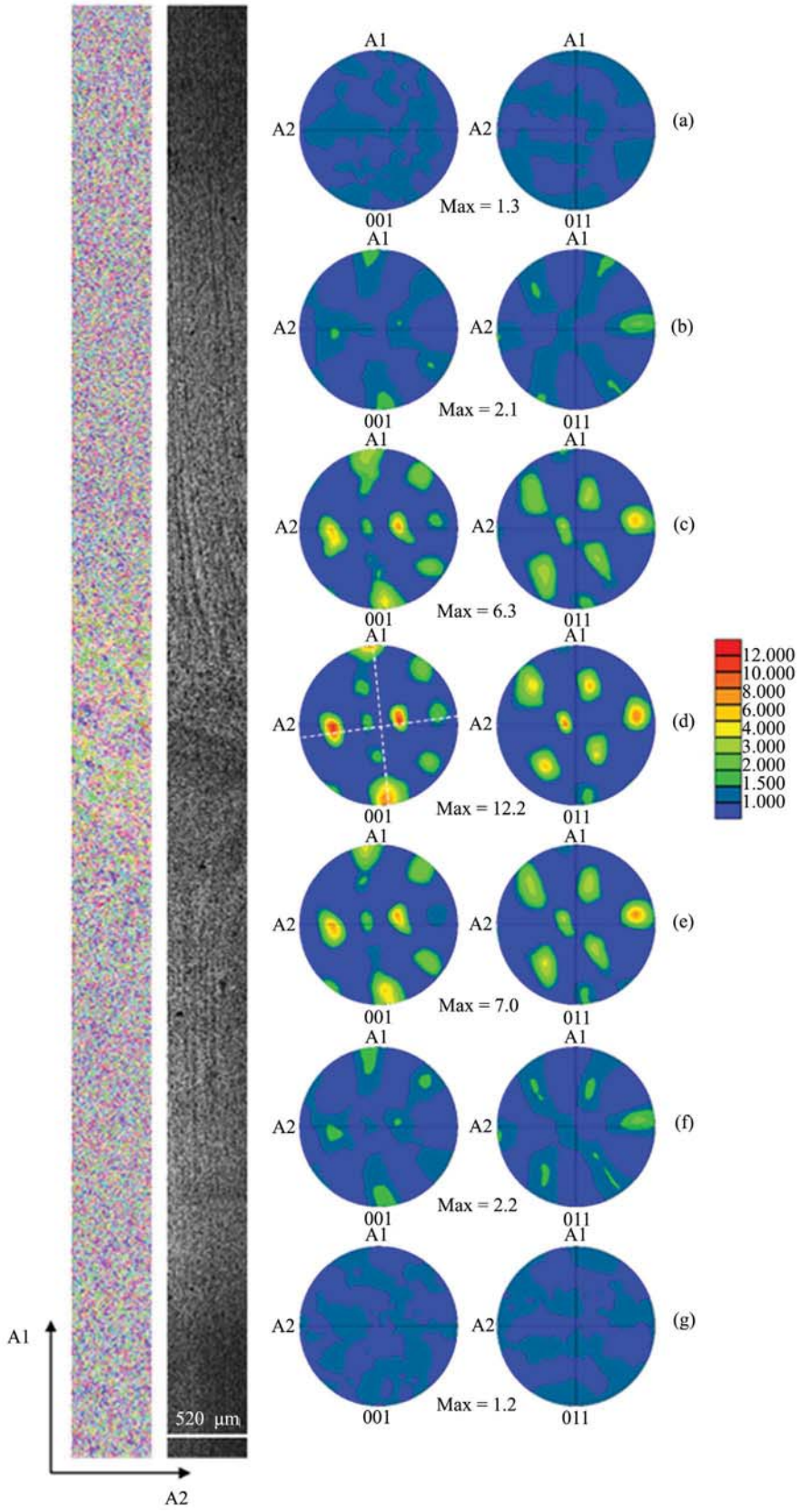

Figure 7. {001}, {011} and {111} pole figures in different sub-zones ((a)-(g)) of the dissimilar welded joint.

The pole figures are rotated with respect to both A1 and A3 axes. The rotation with respect to A1 is constant for all sub-zones which suggests that this rotation is linked to an experimental problem. The rotation relative to A3 increases from the base metal (about 0˚ or a few degrees) to the center of the welded joint (about 10˚). This rotation is related to the production of spiral lines observed in **Figure 4** which indicates the plastic material flow during RFW process [17].

Calculation of the ODF (**Figure 8**) has needed rotations relative to A1 and A3 in order to force texture symmetry and consequently to be able to identify the three main texture components. The texture is essentially composed of the components: Goss {110} <001>, Rotated Cube {100} <110> and Rotated Goss {110} <110>. We consider that the first component (Rotated Cube {100} <110>) is related to the plastic deformation during RFW, because it has been reported that the rotated Cube orientation is important for the development of shear texture components [20]. It has been reported that Rotated cube is stable orientation after cold rolling [21].

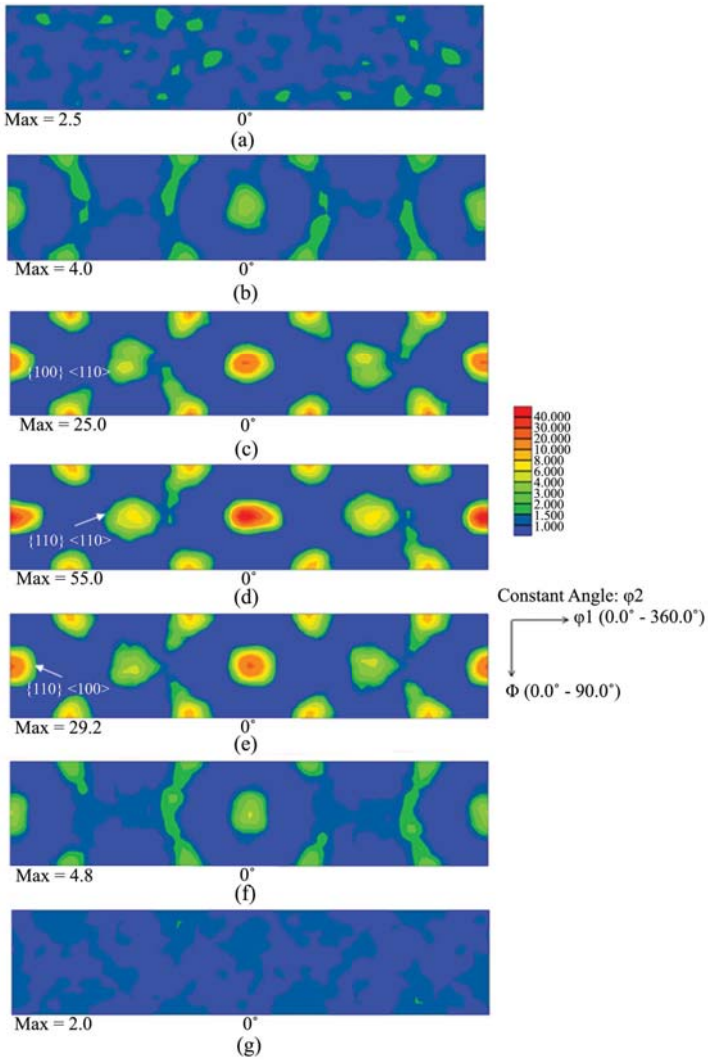

Figure 8. ODF in the welded joint of dissimilar steels (after rotation).

It has been indicted that during subsequent plastic deformation, the crystals rotate toward certain stable orientations. However, Goss {110} <001> and Rotated Goss {110} <110> components are the components of recrystallization. In bcc metals or alloys, the recrystallization textures are largely similar, although the relative prominence of the various texture components may differ to some extent, because of material or processing variations [15]. Our results are in agreement with the finding of Rahimi *et al.* [22]. They found shear deformation with textures ferritic steel side of the two investigated in friction stir welded microalloyed steel. For these reasons cited above, two types of textures were developed in welded joint by FRW; shear (Rotated Cube {100} <110>) and recrystallization textures (Goss {110} <001> and Rotated Goss {110} <110>).

The relative strength of the crystallographic texture was quantified as texture index, a scalar parameter indicating relative anisotropy Engler [23], with a higher value of it signifying strong texture and lower value signifying a random texture.

Figure 9 presents the texture index along the welded joint of dissimilar steels before and after heat treatment at 600˚C (after rotation).The main point is that texture index is higher in the central zone of the welded joint than in the base materials. It is known that the texture gets strengthened when recrystallization occurs. Besides, there is not a significant difference in terms of texture index before and after the heat treatment (**Figure 10**).

Figure 10 presents the texture component fractions in the welded joint of dissimilar steels before after heat treatment at 600˚C (after symmetry correction) with dispersion of 15˚ on the Euler angles. As it is presented in **Figure 10**, there is an increase in the fraction of the components in the two sub-zones (c) and (e) and in the weld (sub-zone d). The Goss fraction is greater than that of the Rotated Cube which is itself greater than that of the Rotated Goss {110} <110> component, while they have similar fractions in the base materials.

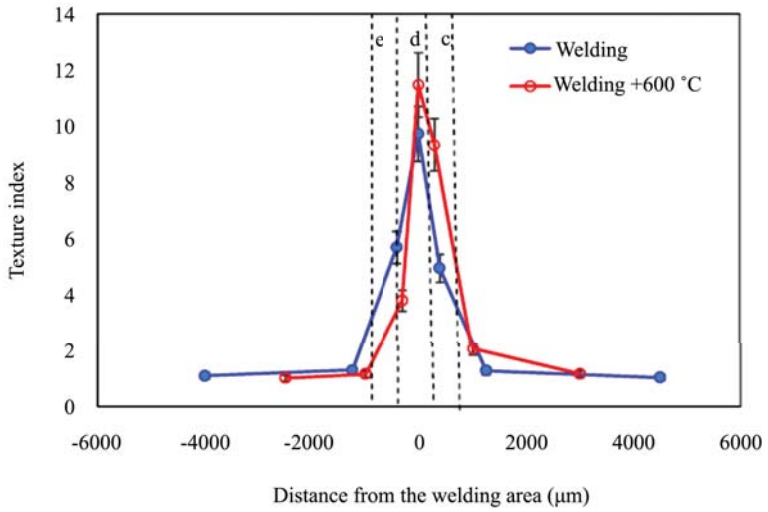

Figure 9. Texture index in the welded joint of dissimilar steels before after heat treatment at 600˚C (after rotation).

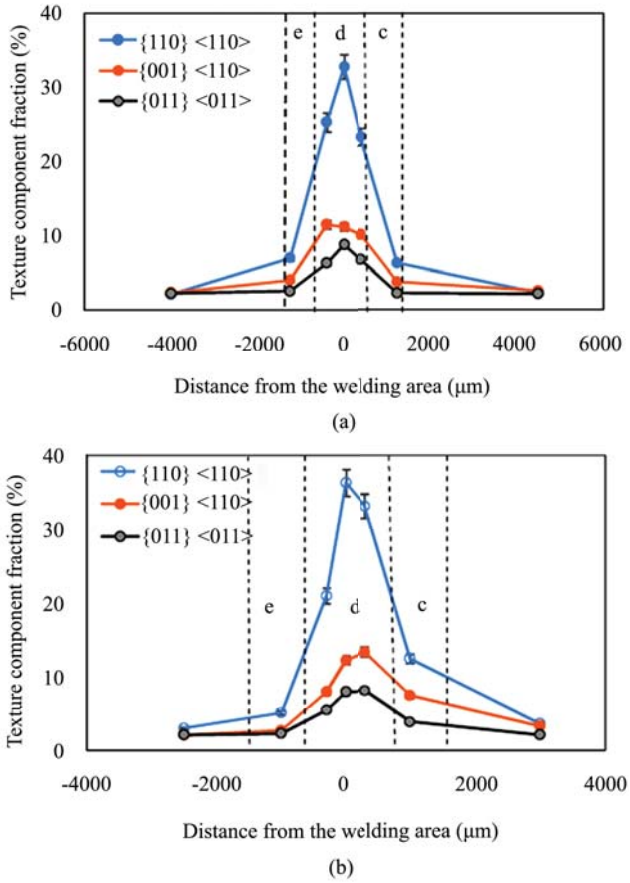

Figure 10. Texture component fraction in the welded joint of dissimilar steels: (a) before and (b) after heat treatment at 600˚C (after rotation).

4. Conclusions

Following conclusions can be drawn from the present work of dissimilar medium carbon steels welded by rotary friction technique.

- The welded joint obtained by RFW is not homogeneous from the microstructural aspect.
- EBSD results revealed that seventh subzones in welded joint and the central zone are different to other zones in terms of texture. The texture in the weld is essentially composed of three components: Goss {110} <001>, Rotated Cube {100} <110>, and Rotated Goss {110} <110> orientation. Rotated Cube {100} <110> is a shear texture; however, Goss {110} <001> and Rotated Goss {110} <110> are recrystallization textures.
- There is not a significant difference between before and after heat treatment at 600˚C in terms of microstructure, texture intensity and texture components whatever the welded zone is studied.

Conflicts of Interest

The authors declare no conflicts of interest regarding the publication of this paper.

References

[1] Zhou, Y., Li, Z., Hu, L., Fuji, A. and North, T.H. (1995) Mechanical Properties of Particulate MMO/AISl304 Friction Joints. *ISIJ International*, **35**, 1315-1321. https://doi.org/10.2355/isijinternational.35.1315

[2] ASM Handbook (1971) Welding, Brazing, and Soldering. 8th Edition, Vol. 6.

[3] Shete, N. and Deokar, S.U. (2017) A Review Paper on Rotary Friction Welding. *International Conference on Ideas, Impact and Innovation in Mechanical Engineering*, **5**, 1557-1560. https://ijritcc.org/download/conferences/ICIIIME_2017/ICIIIME_2017_Track/1498548905_27-06-2017.pdf

[4] Li, W.Y., Vairis, A., Preuss, M. and Ma, T.J. (2016) Linear and Rotary Friction Welding Review. *International Materials Reviews*, **61**, 71-100. https://doi.org/10.1080/09506608.2015.1109214

[5] Maalekian, M. (2007) Friction Welding-Critical Assessment of Literature. *Science and Technology of Welding and Joining*, **12**, 738-759. https://doi.org/10.1179/174329307X249333

[6] Delijaicova, S., Silvaa, P.A.O., Resende, H.B. and Batalhab, M.H.F. (2018) Effect of Weld Parameters on Residual Stress, Hardness and Microstructure of Dissimilar AA2024-T3 and 3AA7475-T761 Friction Stir Welded Joints. *Materials Research*, **21**, 1-11. https://doi.org/10.1590/1980-5373-mr-2018-0108

[7] Cai, W., Daehn, G., Vivek, A., Li, J., Khan, H., Mishra, R.S. and Komarasamy, M. (2019) A State of the Art Review on Solid-State Metal Joining. *Journal of Manufacturing Science and Engineering*, **141**, Article ID: 031012. https://doi.org/10.1115/1.4041182

[8] Radosław, W. (2016) Effect of Friction Welding Parameters on the Tensile Strength and Microstructural Properties of Dissimilar AISI 1020-ASTM A536 Joints. *The International Journal of Advanced Manufacturing Technology*, **84**, 941-955.

[9] Haribabu, S., Cheepu, M., Tammineni, L., Gurasala, N., Devuri, V. and Kantumuchu, V. (2019) Dissimilar Friction Welding of AISI 304 Austenitic Stainless Steel and AISI D3 Tool Steel: Mechanical Properties and Microstructural Characterization. In: *Advances in Materials and Metallurgy*, Springer, Singapore, 271-281. https://doi.org/10.1007/978-981-13-1780-4_27

[10] Zdemira, N.O., Sarsılmaz, F. and Hascalık, A. (2007) Effect of Rotational Speed on the Interface Properties of Friction Welded AISI 304L to 4340 Steel. *Materials and Design*, **28**, 301-307. https://doi.org/10.1016/j.matdes.2005.06.011

[11] Gaikwad, V.T., Mishra, M.K., Hiwarkar, V.D. and Singh, R.K.P. (2020) Microstructure and Mechanical Properties of Friction Welded Carbon Steel (EN24) and Nickel Based Superalloy (IN718). *International Journal of Minerals, Metallurgy and Materials*.

[12] Gan, W., Hofmann, M., Ventzke, V., Randau, C., Huang, Y., Kriele, A., Brokmeier, H.G. and Mueller, M. (2017) Microstructure and Residual Stress in Rotary Friction Welded Dissimilar Metals of AA7020 Aluminum Alloy with 316L Steel. *Materials Science Forum*, **879**, 572-577. https://doi.org/10.4028/www.scientific.net/MSF.879.572

[13] Priymak, E., Atamashkin, A. and Stepanchukova, A. (2019) Effect of Post-Weld Heat Treatment on the Mechanical Properties and Mechanism of Fracture of Joint Welds Made by Thompson Friction Welding. *Materials Today: Proceedings*, **11**, 295-299. https://doi.org/10.1016/j.matpr.2018.12.147

[14] Priymak, E., Boumerzoug, Z., Stepanchukova, A. and Ji, V. (2020) Residual Stresses and Microstructural Features of Rotary-Friction-Welded from Dissimilar Medium C Steels. *The Physics of Metals and Metallography*, **121**, 119-126.

[15] Hu, H. (1974) Texture of Metals. *Texture*, **1**, 233-258. https://doi.org/10.1155/TSM.1.233

[16] Stütz, M., Buzolin, R., Pixner, F., Poletti, C. and Enzinger, N. (2019) Microstructure Development of Molybdenum during Rotary Friction Welding. *Materials Characterization*, **151**, 506-518. https://doi.org/10.1016/j.matchar.2019.03.024

[17] Schwartz, M.M. (1979) Friction Welding, Metals Joining Manual. McGraw-Hill Book Company, New York.

[18] Damodaram, R., Raman, S.G.S. and Rao, K.P. (2013) Microstructure and Mechanical Properties of Friction Welded Alloy 718. *Materials Science and Engineering*: *A*, **560**, 781. https://doi.org/10.1016/j.msea.2012.10.035

[19] Wang, Y., Shao, W.Z., Zhen, L. and Zhang, X.M. (2008) Microstructure Evolution during Dynamic Recrystallization of Hot Deformed Superalloy 718. *Materials Science and Engineering*: *A*, **486**, 321-332. https://doi.org/10.1016/j.msea.2007.09.008

[20] Dhinwal, S.S., Toth, L.S., Hodgson, P.D. and Haldar, A. (2018) Effects of Processing Conditions on Texture and Microstructure Evolution in Extra-Low Carbon Steel During Multi-Pass Asymmetric Rolling. *Materials*, **11**, 1327. https://doi.org/10.3390/ma11081327

[21] Inagaki, H. (1994) Fundamental Aspect of Texture Formation in Low Carbon Steel. *ISIJ International*, **34**, 313-321. https://doi.org/10.2355/isijinternational.34.313

[22] Rahimi, S., Wynne, B.P. and Baker, T.N. (2017) Development of Microstructure and Crystallographic Texture in a Double-Sided Friction Stir Welded Microalloyed Steel. *Journal of Metallurgical and Materials Transactions A*, **48**, 362-378. https://doi.org/10.1007/s11661-016-3833-8

[23] Engler, O. and Randle, V. (2010) Introduction to Texture Analysis, Macrotexture, Microtexture and Orientation Mapping. Second Edition, Taylor and Francis Group, Abingdon-on-Thames. https://doi.org/10.1201/9781420063660